Short-range compositional randomness of hydrogenated amorphous silicon–germanium films

B. D. Chapman and S.-W. Han
Department of Physics, University of Washington, Seattle, Washington 98195-1560

G. T. Seidler[a] and E. A. Stern
Department of Physics, University of Washington, Seattle, Washington 98195-1560 and PNC-CAT Sector 20, Advanced Photon Source, Argonne, Illinois 60439

J. David Cohen
Department of Physics, University of Oregon, Eugene, Oregon 97403

S. Guha and J. Yang
United Solar Systems Corp., 1100 West Maple Road, Troy, Michigan 48084

(Received 12 July 2001; accepted for publication 24 April 2002)

The optical absorption spectrum of hydrogenated amorphous silicon–germanium (a-$Si_{1-x}Ge_x$:H) films can be tuned by the Ge content. As a result, there is considerable interest in applications of this photovoltaic alloy in solar cells. However, some aspects of the relationship between microstructure and optoelectronic properties are not yet fully understood. We report here a study of the local Ge environment in a-$Si_{1-x}Ge_x$:H films having demonstrated high photovoltaic efficiency. We present Ge K-edge extended x-ray absorption fine structure (EXAFS) measurements for samples with Ge content ranging from $x=0.10$ to 0.45. A structural analysis of the EXAFS reveals compositional randomness in the local Ge environment for $x<0.4$, indicating short-range random miscibility of Ge and Si in the alloying process. This is consistent with measurements of earlier generations of Si-rich a-$Si_{1-x}Ge_x$:H films, and suggests that one must look beyond the first coordination shell to understand the relationship between microstructure and optoelectronic properties. We also find no compositional dependence in the Ge environment nearest-neighbor bond lengths, indicating that there is little topological rigidity in the amorphous phase. Together, these results exclude any substantial Ge nanocrystallization or segregation into regions of concentrated Ge hydrides, but do not prohibit more complicated compositional inhomogeneity caused by partial phase separation on longer length scales. © *2002 American Institute of Physics.* [DOI: 10.1063/1.1486037]

I. INTRODUCTION

Amorphous silicon (a-Si) and silicon–germanium alloys (a-$Si_{1-x}Ge_x$) are important semiconductors in microelectronic and photovoltaic device applications, including solar cells, photodetectors, thin film transistors (TFTs), and flat panel displays.[1] In particular, there is considerable interest in hydrogenated amorphous silicon–germanium (a-$Si_{1-x}Ge_x$:H) thin films owing to applications in high efficiency tandem and triple photovoltaic cells.[2,3] The alloying of Ge with a-Si:H lowers the optical band gap, thus improving the photoresponse in the longer wavelength region of the solar spectrum.

Unfortunately, the improved long wavelength response in a-$Si_{1-x}Ge_x$:H films with increasing x often comes at the cost of a significant deterioration in the optoelectronic properties. Characteristics of this degradation include an increase in the density of deep defects, a decrease in carrier mobilities, and a decrease in the photocurrent response.[4] These properties have been attributed to increased occurrence of Ge-dangling bonds,[5] increased size and density of microvoids,[6] and increased film heterogeneity.[7–10] Consequently, a recurring theme during the evolution of deposition techniques in a-$Si_{1-x}Ge_x$ film growth has been the relationship between preparation, microstructure, and physical properties.[7–11]

The problem of compositional inhomogeneity in radio frequency (rf) glow discharge growth of a-$Si_{1-x}Ge_x$:H has received special attention.[6,12–15] Many difficulties which arise in rf glow discharge preparation of a-$Si_{1-x}Ge_x$:H films, such as nonuniform Ge incorporation, are due to the very different decomposition rates of silane (SiH_4) and germane (GeH_4) during film growth. This has been mitigated in two ways: through the use of strong H_2 dilution to modify the surface decomposition rates of both reactants,[16,17] and through the use of disilane (Si_2H_6) instead of SiH_4.[18,19] The latter technique is useful because Si_2H_6 and GeH_4 have similar decomposition rates.[18] Device-quality films grown using both H_2 dilution and also Si_2H_6 substitution for the more common SiH_4 have been included by Yang and coworkers[3] as elements in multijunction, multibandgap solar cells with the highest initial (14.6%) and stable (13.0%) conversion efficiencies to date for a-Si alloy solar cells.

We report here an extended x-ray absorption fine structure (EXAFS) study of rf glow discharge grown

[a]Author to whom correspondence should be addressed; electronic mail: seidler@phys.washington.edu

a-$Si_{1-x}Ge_x$:H films with demonstrated device-quality optoelectronic properties. It is important to note that the a-$Si_{1-x}Ge_x$:H films grown over the past 5 years, such as the samples studied here, are believed to possess a much smaller degree of network disorder than samples prepared a decade ago. In particular, the Urbach energies exhibited by these newer alloy materials have been found to be as low as for pure a-Si:H (below 50 meV), essentially independent of Ge fraction.[6,14] Electronically active deep defect densities are also found to be at least one order of magnitude lower for such materials.[14] An understanding of the new limitations on optoelectronic properties of these improved alloy films requires one to focus on subtle structural issues, such as those studied here.

X-ray absorption fine structure (XAFS), which refers to oscillatory structure in the x-ray absorption coefficient above an x-ray absorption edge, has long been used to study element-specific local atomic structure in crystalline and amorphous systems.[20] XAFS is conventionally divided into the x-ray absorption near-edge structure (XANES) and EXAFS regions, the latter having a typical range of 30 to 1000 eV above the absorption edge. The local structure in $Si_{1-x}Ge_x$ films has been investigated by several groups using the EXAFS technique.[12,13,21–28] EXAFS measurements above the Ge K-edge are able to address two key aspects of the local Ge environment in a-$Si_{1-x}Ge_x$:H films; namely, the alloy compositional dependence of both the near-neighbor coordination number $N_{\mathrm{Ge-Ge}}$ and the Ge constituent near-neighbor bond lengths $R_{\mathrm{Ge-Ge}}$ and $R_{\mathrm{Ge-Si}}$. Modern data analysis methods[29,30] provide now-standard tools for fitting EXAFS data to theoretical standards,[31,32] leading to reliable modeling of the local structure.

Below, we first describe the experimental details and then specify all relevant features of our data analysis. We then present EXAFS results for a-$Si_{1-x}Ge_x$:H with x varying from 0.10 to 0.45. We find that the Ge–Ge first-shell coordination number in the Si-rich films ($x<0.4$) is fully consistent with a completely random local environment. We also find no Ge concentration dependence in the Ge–Ge or Ge–Si bond lengths. Before concluding, we discuss two aspects of these results. First, we compare and contrast our results with those from previous EXAFS studies of films with various preparations. Second, we address the extent to which our results exclude subtle concentration segregation on larger length scales.

II. EXPERIMENT

Sample preparation is described in detail elsewhere.[33] Briefly, the a-$Si_{1-x}Ge_x$:H films were deposited onto single crystal Si substrates at $T\sim 300\,^{\circ}\mathrm{C}$ by rf glow discharge decomposition of H_2, GeH_4, and Si_2H_6. We report EXAFS measurements of five samples, with Ge content $x=0.452$, 0.325, 0.202, 0.13, and 0.10. Energy dispersive spectroscopy (EDS) measurements were carried out in order to measure the Ge content in the three highest concentration films, with an absolute uncertainty in the atomic fraction of 0.002. Auger depth profile measurements were made to determine the Si content in the two lowest Ge concentration films, with an absolute uncertainty in the atomic fraction of 0.01. The film thicknesses are, in order of decreasing Ge content, 1.05, 1.24, 1.19, 1.1, and 1.1 μm. IR spectroscopy of equivalently prepared films found about 12% hydrogen bonded in Si–H or Ge–H bonds.[34] Films from the same deposition conditions and in some cases the same substrate wafers have previously been characterized by a wide range of measurements, including drive level capacitance profiling, transient photocapacitance, and junction transient photocurrent methods.[5,35] These studies all establish low defect densities in the films and device-quality optoelectronic properties.

All measurements were performed at the Pacific Northwest Consortium Collaborative Access Team (PNC-CAT) bending magnet beamline (20-BM) at the Advanced Photon Source x-ray synchrotron located at Argonne National Laboratory.[36] Energy selection was achieved using a water-cooled double crystal Si(111) monochromator. Harmonic rejection was achieved either by detuning the monochromator 30% or by the use of a Rh-coated harmonic rejection mirror. The beam height was 1.5 mm, yielding an energy resolution of $\sim$1.5 eV. The beam width was varied between 1.0 and 3.0 mm depending on the sample measured. The incident beam was horizontally polarized. The incident flux, I_0, was monitored with a N_2-filled ionization chamber. The fluorescence yield from the sample, I_F, was measured with a low-noise ionization chamber filled with a N_2/Ar gas mixture. The sample and detector were oriented symmetrically at 45° and 90°, respectively, with respect to the incoming beam.

The small sample thickness compared to the x-ray absorption length together with the strong elastic scattering cross-section from the single crystal Si substrates required several measures to minimize contamination of the EXAFS signal. These included spinning the samples at $\sim$500 rpm to rotationally average the diffraction background, using a Ga filter and line-focusing Soller slits,[37] using a horizontal experimental geometry with a scattering angle near 90° to decrease dipole scattering, and masking Bragg peaks at the detector face with 1 mm thick Pb tape.

III. DATA ANALYSIS

The EXAFS is analyzed using the UWXAFS software package.[30] Background subtraction is achieved using AUTOBK[29] through the relation

$$\chi(E)=\frac{\mu(E)-\mu_0(E)}{\Delta\mu_0(E_0)}, \tag{1}$$

where E_0 is the absorption edge energy, $\mu_0(E)$ is the expected smooth atomic absorption past the edge in the absence of photoelectron backscattering, and $\Delta\mu_0(E_0)$ is the absorption jump at the edge. The term $\mu_0(E)$ is approximated by a piecewise spline, optimized to reduce the nonstructural components in the Fourier transform for radial distances less than 1.3 Å. The function $\chi(E)$ is interpolated into k space, $\chi(k)$, where $k=\sqrt{2m(E-E_0)/\hbar^2}$ is the momentum of the photoelectron. The program ATOMS[29] provides corrections to the Debye–Waller factors resulting from the edge-step normalization of $\chi(k)$ and the different energy responses of the two measured signals, I_F and I_0.

TABLE I. The structural parameters found in the EXAFS global fit for each of the five a-$Si_{1-x}Ge_x$:H films measured as a function of Ge content x. Also shown are the Fourier transform properties and R-space fitting parameters for each data set. The Debye–Waller factors $\sigma^2(x)$ are found to be independent of alloy composition. N_{Ge-Si} is the first-shell coordination number of Si atoms, with bond length R_{Ge-Si}.

x	k_{min} (Å^{-1})	k_{max} (Å^{-1})	R_{min} (Å)	R_{max} (Å)	σ^2 (Å^2)	N_{Ge-Ge}	N_{Ge-Si}	R_{Ge-Ge} (Å)	R_{Ge-Si} (Å)
0.452	3.3	14.0	1.59	2.80	0.0039(05)	2.01(13)	1.99(13)	2.462(04)	2.389(14)
0.325	3.3	15.0	1.57	2.80	0.0041(07)	1.36(19)	2.64(19)	2.461(08)	2.392(19)
0.202	3.3	12.0	1.66	2.80	0.0041(17)	0.68(36)	3.32(36)	2.469(43)	2.393(39)
0.13	3.3	14.0	1.69	2.80	0.0034(15)	0.52(31)	3.48(31)	2.460(45)	2.406(27)
0.10	3.3	11.5	1.71	2.80	0.0039(15)	0.42(33)	3.58(33)	2.473(57)	2.396(28)

Structural information is extracted from the measured EXAFS signal through the relationship for unpolarized K-shell absorption processes,[38]

$$\chi(k)=\sum_j S_0^2 N_j \frac{F_j(k)}{kR_j^2}\exp(-2k^2\sigma_j^2)\exp[-2R_j\lambda_j^{-1}(k)] \times \sin[2kR_j+\phi_j(k,R_j)], \quad (2)$$

where only the single-scattering photoelectron contributions are important for single coordination shell systems. $F_j(k)$, $\phi_j(k)$, and $\lambda_j(k)$ are the photoelectron backscattering amplitude, phase, and mean-free-path factor, respectively, for path j that are generated from the *ab initio* calculations of the FEFF7 code.[32] The backscattering atoms, either Ge or Si, distinguish the path j in the summation. The remaining terms in Eq. (2) are the coordination number N_j, the coordination shell bond length R_j, and the Debye–Waller factor σ_j^2. The latter term represents the mean-square variation in R_j due to both static and thermal disorder. Anharmonic corrections are expected to be negligible and have been ignored.

The structural parameters in $\chi(k)$ were determined using FEFFIT,[30] which employs a nonlinear, least-squares fit to the theoretical standards calculated by FEFF7. We also vary a single nonstructural parameter E_0 independently for each sample concentration. A *global* fit was performed in order to create a single concentration independent passive electron core hole factor parameter S_0^2 for the entire data set. The uncertainties reported by FEFFIT are underestimated in the global fit. We have therefore rescaled the parameter uncertainties reported by FEFFIT to reflect the true number of degrees of freedom in each respective data set. The self-absorption effect has a non-negligible effect on the measured EXAFS amplitudes, resulting in a 5% reduction in the amplitude of the highest Ge concentration film measured.[39] Appropriate amplitude correction factors for each data set were included in the fit. Fourier transforms to R space were done using k^2 weighting and Hanning windows, over a range of $k_{min}=3.3$ Å^{-1} up to the end of the data, typically $k_{max}\sim 14$ Å^{-1}. The data were fit in R space in the range $R_{min}\sim 1.6$ Å to $R_{max}=2.80$ Å, with R_{min} varying accordingly with k_{max}. These details are contained in Table I.

Two constraints were imposed in the structural model. First, the two contributing Debye–Waller factors (σ^2_{Ge-Ge} and σ^2_{Ge-Si}) were set equal to each other for each alloy composition. The equivalency of the fluctuations in the Ge–Ge and Ge–Si bond lengths has been demonstrated in SiGe alloys by prior EXAFS investigations.[12,24,27,28] The physical reasoning behind this assumption follows from the similar Keating potentials computed in pure Si and Ge.[40] Second, the total coordination number was fixed at four. This assumption is justified by the strongly covalent bonding and resulting local tetrahedral structure of a-Si (Ref. 41) and a-Ge,[42] and it has been shown to be valid even in films with considerable hydrogenation.[12,41–44] We do not find any improvement in our structural model if we decrease the total coordination number in order to allow for dangling bonds or substitutional binding of hydrogen atoms in the local Ge environment. Relaxing either of these fitting constraints confirmed their validity within the experimental uncertainties and does not affect our conclusions.

IV. RESULTS

We show in Fig. 1 the raw fluorescence signal measured as a function of incoming photon energy near the Ge K-edge (11 105 eV) for the $x=0.452$ sample. The effective fluorescent signal was typically $\sim 10^6$ photons/s, and EXAFS spectra with high signal-to-noise ratios were obtained in a few hours per sample. Figure 2 shows the k^2-weighted EXAFS spectra after background subtraction for each of the five

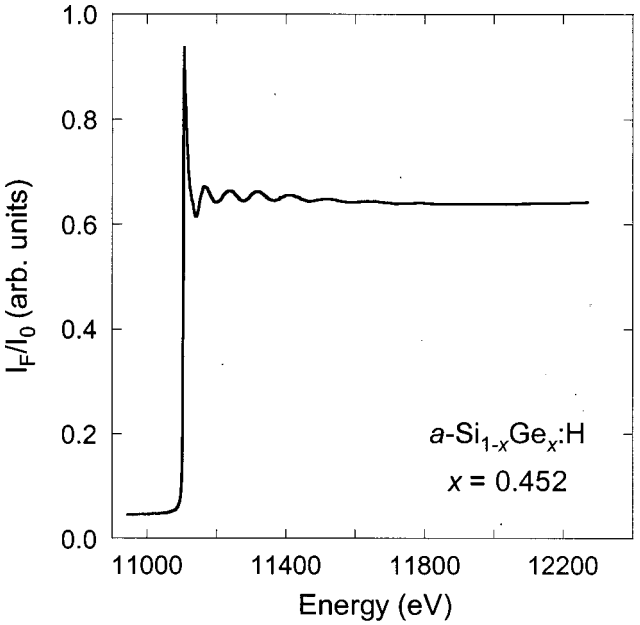

FIG. 1. Raw data. The Ge K-edge fluorescent XAFS signal from the $x=0.452$ a-$Si_{1-x}Ge_x$:H film.

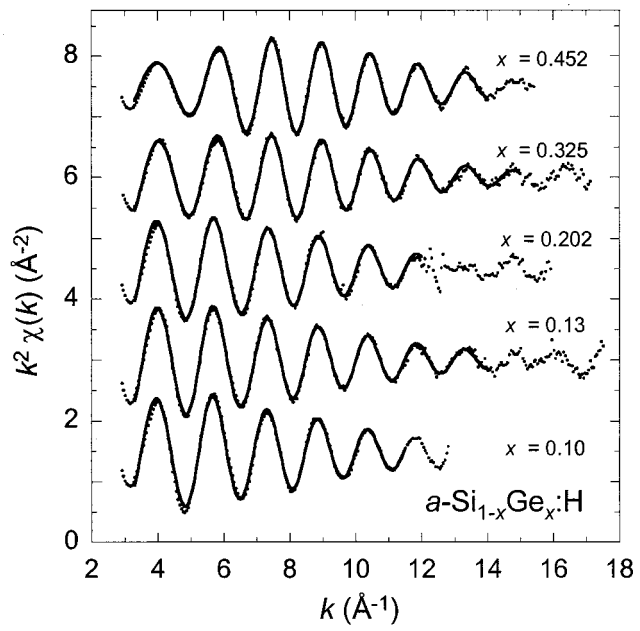

FIG. 2. The k^2-weighted EXAFS spectra and the Fourier transforms of the corresponding fits for the five a-$Si_{1-x}Ge_x$:H films, each shifted vertically for clarity of viewing. The dots are the data, and the solid lines are the Fourier transforms of the fits found in R space. The glitches that appear in the high k regions of the data result from diffraction effects from the sample substrate; these regions were excluded in the analysis. Note the differences in the signal envelope with alloy composition resulting from the distinct Ge and Si scattering cross-sections.

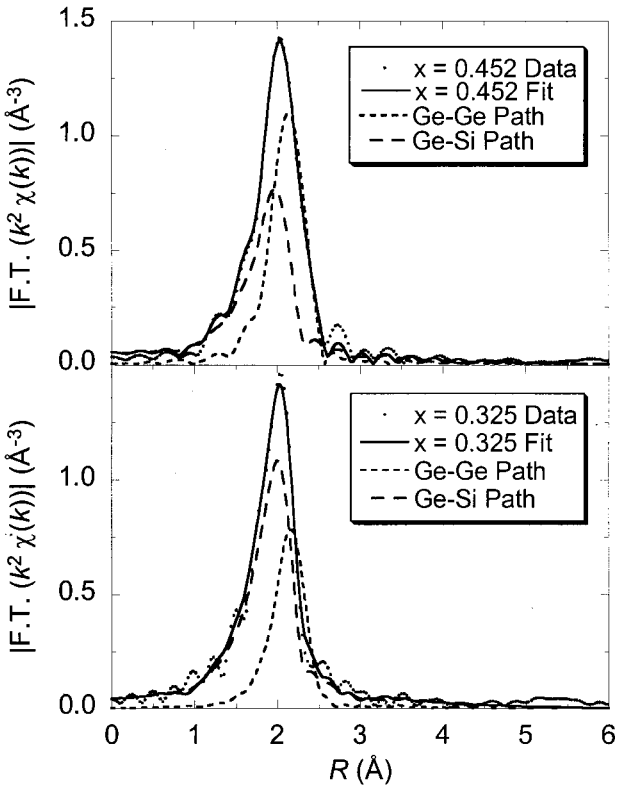

FIG. 3. The magnitude of the Fourier transformed k^2-weighted data (dots) shown for the $x=0.452$ (top) and $x=0.325$ (bottom) EXAFS. The dashed lines are the individual single-scattering path fits to the data, and the solid lines are the complete fits after path summation. Note that there is no structure for $R>3.0$ Å, and therefore no evidence for significant microcrystalline growth of Ge atoms.

samples (dots), along with the Fourier transforms of the fits from FEFFIT (solid lines). The spectral extent of the data was primarily limited by Bragg scattering from the substrates and varies from sample to sample. Note that there is essentially only one frequency in the signal, indicating that there is only one coordination shell around the core Ge atoms. This is due to the large disorder in bond angles and has been observed in prior EXAFS studies of a-Ge[42,43] and a-$Si_{1-x}Ge_x$.[12,22,28] Also note the shift of the envelope function maximum to a lower wave number with decreasing Ge content. The Ge–Si single-scattering path has an EXAFS signal envelope peaked at a lower wave number compared to the Ge–Ge single-scattering path. Consequently, the dependence of the Ge environment coordination number with alloy composition is qualitatively apparent.[12]

Table I contains the important results of the structural modeling. The total number of variables in the global fit is 26, allowing 19 degrees of freedom in the fitting of the 45 independent data points. The good agreement between theory and experiment together with the physically reasonable values for S_0^2 (0.92 ± 0.05) and $\sigma^2(x)$ gives us high confidence in the fits. The Debye–Waller factors are found to be independent of alloy composition within the uncertainty (see Table I), with a weighted mean of $\overline{\sigma^2}(x)=0.0040\pm0.0004$ Å^2. Figure 3 displays the magnitude of the Fourier transform (dots) as a function of real space separation R for two different alloy concentrations, $x=0.452$ and 0.325. The two peaks corresponding to the near-neighbor bond lengths (Ge–Ge and Ge–Si) are not separated because of the small difference in the bond distance. The dashed lines in the figure are the fits for the two distinct scattering paths, and the solid line is the total fit after path summation. The lack of any signal at distances $R>3.0$ Å excludes any appreciable microcrystallinity in the Ge environments.

Figure 4 shows the resulting Ge–Ge coordination numbers as a function of Ge alloy fraction x. The reported uncertainties in the coordination numbers are about ten times larger than the random fluctuations in the data. This indicates that the experiment is dominated by systematic errors, which is typical of EXAFS modeling. Consequently, the relative variation of the data points is much more reliable than what is indicated by the error bars. Systematic errors, with the exception of the self-absorption effect, are expected to be independent of alloy composition. We therefore expect errors in the Si-rich data points to be biased collectively. The results of the Ge environment coordination number for $x<0.4$ are quite consistent with a random local distribution of the Ge atoms, indicated by the straight line in Fig. 4.

In Fig. 5 we show the near-neighbor bond lengths as a function of x, along with their respective linear regression lines. Both bond lengths are found to be independent of alloy composition, with linear slopes of $m_{\mathrm{Ge-Ge}}=-0.003\pm0.058$ and $m_{\mathrm{Ge-Si}}=-0.034\pm0.069$ and weighted means of $\overline{R}_{\mathrm{Ge-Ge}}=2.462\pm0.004$ Å and $\overline{R}_{\mathrm{Ge-Si}}=2.393\pm0.009$ Å.

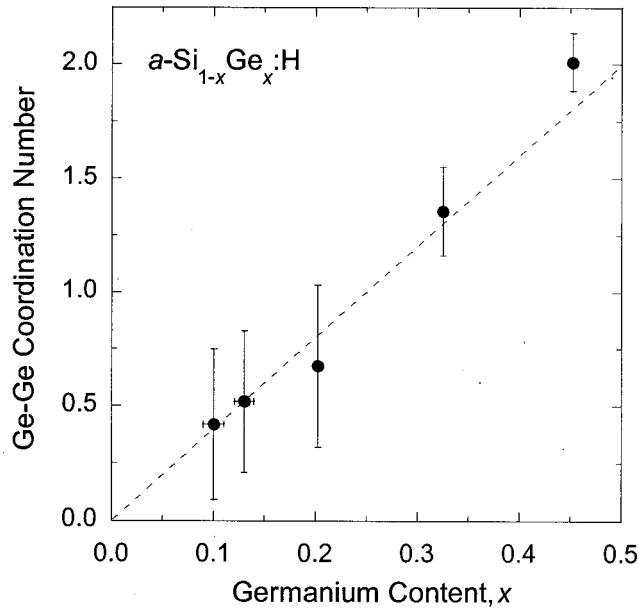

FIG. 4. Ge–Ge coordination number as a function of the Ge fraction x. The dashed line is the expected result for complete short-range compositional randomness when the total coordination for each Ge atom is four. The relative uncertainties in the coordination numbers are much smaller than the error bars shown, indicating that the experiment is dominated by systematic errors. The uncertainties in the concentration for the three highest Ge content samples are smaller than the symbol size.

V. DISCUSSION

We now compare and contrast our results with those from previous studies. This will take three parts. First, we discuss short-range compositional ordering, carefully comparing our results with those of previous investigations. Second, we discuss the behavior of the species-specific bond lengths, $R_{\mathrm{Ge-Ge}}$ and $R_{\mathrm{Ge-Si}}$, in the context of theories of the topological rigidity of amorphous alloys. Finally, before concluding, we address the possibility of more complicated sample heterogeneity, for example, by partial phase separation on longer length scales than are probed by EXAFS.

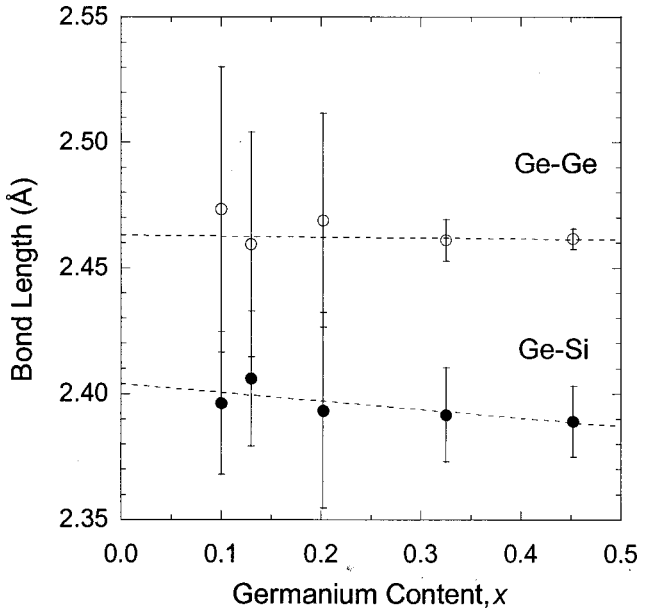

FIG. 5. The Ge–Ge and Ge–Si near-neighbor bond lengths in a-$Si_{1-x}Ge_x$:H films as a function of x. The nonzero slopes of the linear least-squares fits to the data, shown by the dashed lines, are not statistically significant. Consequently, to within experimental error the bond lengths are independent of alloy composition.

First, the simplest heterogeneity that can exist in even an equilibrium system is compositional clustering in the first coordination shell. As summarized in Table II, this topic has been addressed in several EXAFS studies of both a-$Si_{1-x}Ge_x$ and c-$Si_{1-x}Ge_x$ samples with a variety of different preparations. Over the relevant range of x our work is in good agreement with the work of Nishino *et al.*[13] In that study, a 20% excess in the Ge–Ge coordination number was reported for $x=0.47$, which used a qualitatively similar sample preparation as in the present study but unfortunately had no information about the possible device quality of the films. By comparison, our sample with $x=0.45$ shows a 11% excess in Ge–Ge coordination, but it should be emphasized that this is only a 1.6σ effect [$P_G(\mu+1.6\sigma)=0.11$], where the error is likely dominated by the self-absorption effect. Our results extend the range of compositional randomness in Si-rich glow discharge a-$Si_{1-x}Ge_x$:H films down to $x=0.10$. To within the errors inherent to EXAFS analysis, we conclude that first-shell compositional randomness is a general property of Si-rich glow discharge a-$Si_{1-x}Ge_x$:H films grown with H_2 dilution and Si_2H_6 as a reactant gas for $x<0.4$. Due to the high sample preparation temperature, it is not immediately clear how to compare our results with the simulations of Tzoumanekas and Kelires,[45] who argue that at low sample preparation temperatures the bond-length differences in the system drive short-range segregation but stabilize long-range compositional homogeneity at all Ge concentrations.

Second, the competition between bond-length and bond-angle rigidity in amorphous binary alloys is a topic of continuing interest for theory and simulation.[46–48] Our results, i.e., demonstrating the absence of bond-length variation with x, are in agreement with all previous experimental studies of glow discharge a-$Si_{1-x}Ge_x$:H. This means that a-$Si_{1-x}Ge_x$:H exhibits little topological rigidity, i.e., local stresses are accommodated by changing bond angles rather than bond lengths. It should be noted that Ridgway *et al.*,[28] whose samples were prepared by amorphization of c-$Si_{1-x}Ge_x$ layers grown by molecular beam epitaxy (MBE), found evidence for a weak composition dependence in $R_{\mathrm{Ge-Ge}}$ over their full range of concentrations, but that this dependence was not statistically significant for the subset of samples with $x<0.5$.

Finally, it is important to recognize that there are many types of inhomogeneity which may influence device performance, of which first-shell compositional segregation is only the simplest. In this context, we restrict ourselves to discuss only a recent careful study by Goerigk and Williamson[15] of anomalous small angle x-ray scattering from a-$Si_{1-x}Ge_x$:H films prepared by glow discharge with H_2 dilution and appropriate SiH_4/GeH_4 mixtures. The results were interpreted as evidence for two-phase segregation, with a small increase in Ge content in the dominant phase with a columnar microstructure in the growth direction and a considerable decrease

TABLE II. A summary of the significant results from the EXAFS studies of amorphous and crystalline $Si_{1-x}Ge_x$ films with various preparation methods. A preparation listed simply as "glow discharge" means that SiH_4 and GeH_4 were used without H_2 dilution. The bond lengths in question are the nearest-neighbor bond lengths.

Study	Sample	Sample preparation	First-shell randomness?	Bond-length variation?
Incoccia *et al.* (1985)[a]	a-$Si_{1-x}Ge_x$:H $0.29 \leqslant x \leqslant 0.9$	glow discharge	yes	no
Filipponi *et al.* (1986)[b]	a-$Si_{1-x}Ge_x$:H $0.17 \leqslant x \leqslant 0.80$	glow discharge	yes	no
Nishino *et al.* (1988)[c]	a-$Si_{1-x}Ge_x$:H $0.27 \leqslant x \leqslant 0.56$	glow discharge, with H_2 and Si_2H_6	yes ($x<0.47$) no ($x>0.47$)	no
Ridgway *et al.* (1999)[d]	a-$Si_{1-x}Ge_x$ $0.04 \leqslant x \leqslant 1.0$	MBE+Si ion implantation	(assumed)	yes
Present study	a-$Si_{1-x}Ge_x$:H $0.10 \leqslant x \leqslant 0.45$	glow discharge, with H_2 and Si_2H_6	yes ($x<0.4$) no ($x=0.45$)	no
Kajiyama *et al.* (1992)[e]	c-$Si_{1-x}Ge_x$ $0.20 \leqslant x \leqslant 1.0$	glow discharge+anneal, with H_2 and Si_2H_6	yes	no
Aldrich *et al.* (1994)[f]	c-$Si_{1-x}Ge_x$ $0.36 \leqslant x \leqslant 0.82$	MBE	yes	yes
Aubry *et al.* (1999)[g]	c-$Si_{1-x}Ge_x$ $0 \leqslant x \leqslant 0.95$	MBE	yes ($x>0.1$) no ($x<0.1$)	yes
Ridgway *et al.* (1999)[d]	c-$Si_{1-x}Ge_x$ $0.04 \leqslant x \leqslant 1.0$	MBE	(assumed)	yes

[a]Reference 12.
[b]Reference 22.
[c]Reference 13.
[d]Reference 28.
[e]Reference 25.
[f]Reference 24.
[g]Reference 27.

in local Ge content in the remaining ~5%–10% of the sample interstitial between the columnar regions. Unfortunately, this type of two-phase model is difficult if not impossible to resolve with EXAFS. The concentration increase in the high-volume phase is within our experimental errors, and the low-volume phase with greatly decreased Ge content would have little weight in our fluorescence measurement. Consequently, it is important to realize that our Si-rich results demonstrate first-shell compositional randomness in a one-phase system, but do not noticeably constrain more complicated inhomogeneity coupled to partial phase separation on longer length scales.

VI. CONCLUSIONS

We have used EXAFS to study the local atomic structure in device-quality a-$Si_{1-x}Ge_x$:H films grown under optimized conditions with both H_2 dilution and Si_2H_6 as a reactant gas. We find no composition dependence in the bond lengths, indicating that there is little topological rigidity in the amorphous phase. Assuming a single phase, we find no evidence of Ge–Ge clustering for alloy compositions in the range $x=0.1-0.4$. However, we are unable to rule out the possibility of subtle clustering on longer length scales associated with phase separation. These results suggest that one must look beyond the first coordination shell to understand the relationship between microstructure and optoelectronic properties in a-$Si_{1-x}Ge_x$:H films.

ACKNOWLEDGMENTS

The authors thank J. O. Cross, S. M. Heald, R. A. Gordon, D. L. Brewe, M. Newville, and D. Haskel for useful discussions and technical assistance. The authors also thank B. Chao for Auger measurements. This research was partially supported by the U.S. Department of Energy, Basic Energy Sciences, under Contract No. DE-FG03-97ER45628 and Contract No. DE-FG07-97ER14818. PNC-CAT is supported by the U.S. Department of Energy, Basic Energy Sciences, under Contract No. DE-FG03-97ER45628, the University of Washington, and grants from the Natural Sciences and Engineering Research Council of Canada. Use of the Advanced Photon Source was supported by the U.S. Department of Energy, Basic Energy Sciences, Office of Science, under Contract No. W-31-109-Eng-38. Work at United Solar was partially supported by the National Renewable Energy Laboratory under Subcontract No. ZAK-8-17619-09. G.T.S. acknowledges support from the Research Corporation as a Cottrell Scholar.

[1] *Amorphous and Microcrystalline Silicon Technology*, edited by R. Schropp, H. M. Branz, M. Hack, I. Shimizu, and S. Wagner, *MRS Symposia Proceedings No. 507* (Materials Research Society, Warrendale, PA, 1999); *Amorphous and Microcrystalline Semiconductor Devices: Optoelectronic Devices*, edited by J. Kanicki (Artech House, Boston, 1991); *Amorphous Semiconductors for Microelectronics*, edited by D. Adler (SPIE, Bellingham 1986).
[2] *Properties of Amorphous Silicon and Its Alloys*, EMIS Datareviews Series No. 19, edited by T. Searle (INSPEC, London, 1998).
[3] J. Yang, A. Banerjee, and S. Guha, Appl. Phys. Lett. **70**, 2975 (1997).
[4] See, for example, J. D. Cohen, in *Properties of Amorphous Silicon and Its*

Alloys, EMIS Datareviews Series No. 19, edited by T. Searle (INSPEC, London, 1998), pp. 180–187, and references therein.
[5] K. C. Palinginis, J. D. Cohen, J. C. Yang, and S. Guha, J. Non-Cryst. Solids **266–269**, 665 (2000).
[6] S. Guha, J. Yang, S. J. Jones, Y. Chen, and D. L. Williamson, Appl. Phys. Lett. **61**, 1444 (1992).
[7] K. D. Mackenzie, J. R. Eggert, D. J. Leopold, Y. M. Li, S. Lin, and W. Paul, Phys. Rev. B **31**, 2198 (1985).
[8] K. D. Mackenzie, J. H. Burnett, J. R. Eggert, Y. M. Li, S. Lin, and W. Paul, Phys. Rev. B **38**, 6120 (1988).
[9] S. J. Jones, Y. Chen, D. L. Williamson, R. Zedlitz, and G. Bauer, Appl. Phys. Lett. **62**, 3267 (1993).
[10] D. L. Williamson, Mater. Res. Soc. Symp. Proc. **377**, 251 (1995).
[11] F. Finger and W. Beyer, in *Properties of Amorphous Silicon and Its Alloys*, EMIS Datareviews Series No. 19, edited by T. Searle (INSPEC, London, 1998), pp. 20–29.
[12] L. Incoccia, S. Mobilio, M. G. Proietti, P. Fiorini, C. Giovannella, and G. Evangelisti, Phys. Rev. B **31**, 1028 (1985).
[13] Y. Nishino, S. Muramatsu, Y. Takano, and H. Kajiyama, Phys. Rev. B **38**, 1942 (1988).
[14] P. Wickboldt, D. Pang, W. Paul, J. H. Chen, F. Zhong, C.-C. Chen, J. D. Cohen, and D. L. Williamson, J. Appl. Phys. **81**, 6252 (1997).
[15] G. Goerigk and D. L. Williamson, J. Non-Cryst. Solids **281**, 181 (2001).
[16] J. Yang, A. Banerjee, T. Glatfelter, K. Hoffman, X. Xu, and S. Guha, *IEEE First World Conference on Photovoltaic Energy Conversion* (IEEE, New York, 1994), Vol. 1, pp. 380–385.
[17] A. R. Middya, S. Ray, S. J. Jones, and D. L. Williamson, J. Appl. Phys. **78**, 4966 (1995).
[18] S. Guha, J. Non-Cryst. Solids **77–78**, 1451 (1985).
[19] A. Matsuda and G. Ganguly, Appl. Phys. Lett. **67**, 1274 (1995).
[20] *X-ray Absorption: Principles, Applications, Techniques of EXAFS, SEXAFS, and XANES*, edited by D. C. Koningsberger and R. Prins (Wiley, New York, 1988).
[21] S. Minomura, K. Tsuji, M. Wakagi, T. Ishidate, K. Inoue, and M. Shibuya, J. Non-Cryst. Solids **59 & 60**, 541 (1983).
[22] A. Filipponi, P. Fiorini, F. Evangelisti, A. Balerna, and S. Mobilio, J. Phys. (Paris), Colloq. **8**, 357 (1986).
[23] M. Matsuura, J. M. Tonnerre, and G. S. Cargill, Phys. Rev. B **44**, 3842 (1991).
[24] D. B. Aldrich, R. J. Nemanich, and D. E. Sayers, Phys. Rev. B **50**, 15026 (1994).
[25] H. Kajiyama, S.-i Muramatsu, T. Shimada, and Y. Nishino, Phys. Rev. B **45**, 14005 (1992).
[26] J. C. Woicik, K. E. Miyano, C. A. King, R. W. Johnson, J. G. Pelligrino, T.-L. Lee, and Z. H. Lu, Phys. Rev. B **57**, 14592 (1998).
[27] J. C. Aubry, T. Tyliszczak, A. P. Hitchcock, J.-M. Baribeau, and T. E. Jackman, Phys. Rev. B **59**, 12872 (1999).
[28] M. C. Ridgway, K. M. Yu, C. J. Glover, G. J. Foran, C. Clerc, J. L. Hansen, and A. N. Larsen, Phys. Rev. B **60**, 10831 (1999).
[29] M. Newville, P. Livins, Y. Yacoby, J. J. Rehr, and E. A. Stern, Phys. Rev. B **47**, 14126 (1993).
[30] E. A. Stern, M. Newville, B. Ravel, Y. Yacoby, and D. Haskel, Physica B **208&209**, 117 (1995).
[31] J. J. Rehr and R. C. Albers, Rev. Mod. Phys. **72**, 621 (2000).
[32] A. Ankudinov and J. J. Rehr, Phys. Rev. B **56**, R1712 (1997).
[33] S. Guha, J. S. Payson, S. C. Agarwal, and S. R. Ovshinsky, J. Non-Cryst. Solids **97–98**, 1455 (1987).
[34] A. H. Mahan, J. Yang, S. Guha, and D. L. Williamson, Phys. Rev. B **61**, 1677 (2000).
[35] C.-C. Chen, F. Zhong, J. D. Cohen, J. C. Yang, and S. Guha, Phys. Rev. B **57**, R4210 (1998).
[36] S. M. Heald, D. L. Brewe, E. A. Stern, K. H. Kim, F. C. Brown, D. T. Jiang, E. D. Crozier, and R. A. Gordon, J. Synchrotron Radiat. **6**, 347 (1999).
[37] E. A. Stern and S. M. Heald, Rev. Sci. Instrum. **50**, 1579 (1979).
[38] E. A. Stern and S. M. Heald, in *Handbook on Synchrotron Radiation*, edited by E. E. Koch (North-Holland, New York, 1983), Vol. 1, pp. 955–1014.
[39] Z. Tan, J. I. Budnick, and S. M. Heald, Rev. Sci. Instrum. **60**, 1021 (1989).
[40] P. N. Keating, Phys. Rev. **145**, 637 (1966).
[41] A. Menelle, A. M. Flank, P. Lagarde, and R. Bellissent, J. Phys. (Paris), Colloq. **8**, 379 (1986).
[42] C. E. Bouldin, E. A. Stern, B. von Roedern, and J. Azoulay, Phys. Rev. B **30**, 4462 (1984).
[43] E. D. Crozier, in *EXAFS Spectroscopy*, edited by B. K. Teo and D. C. Joy (Plenum, New York, 1981), pp. 89–103.
[44] L. Incoccia and S. Mobilio, in *EXAFS and Near Edge Structure III*, edited by K. O. Hodgson, B. Hedman, and J. E. Penner-Hahn (Springer-Verlag, New York, 1984), pp. 284–286.
[45] C. Tzoumanekas and P. C. Kelires, Phys. Rev. B **60**, 14205 (1999); J. Non-Cryst. Solids **266–269**, 670 (2000).
[46] N. Mousseau and M. F. Thorpe, Phys. Rev. B **46**, 15887 (1992).
[47] H. Rucker and M. Methfessel, Phys. Rev. B **52**, 11059 (1995).
[48] J. Shen, J. Zi, X. Xie, and P. Jiang, Phys. Rev. B **56**, 12084 (1997).